The effects of growth phase and salinity on the hydrogen isotopic composition of alkenones produced by coastal haptophyte algae

David Chivall*, Daniela M'Boule, Daniëlle Sinke-Schoen, Jaap S. Sinninghe Damsté, Stefan Schouten, Marcel T.J. van der Meer

NIOZ Royal Netherlands Institute for Sea Research
Department of Marine Organic Biogeochemistry
PO Box 59
1790 AB Den Burg
Netherlands

*Corresponding author. Tel.: +31222369409
Email address: david.chivall@nioz.nl

Geochimica et Cosmochimica Acta 140 (2014), 381-390. doi:10.1016/j.gca.2014.05.043

The hydrogen isotope data used in this manuscript are available at
http://doi.pangaea.de/10.1594/PANGAEA.832256

The alkenone abundance and distribution data used in this manuscript are available at
http://doi.pangaea.de/10.1594/PANGAEA.823603

Supplementary data associated with this article can be found at
http://doi.org/10.1016/j.gca.2014.05.043

Abstract

The isotopic fractionation of hydrogen during the biosynthesis of alkenones produced by marine haptophyte algae has been shown to depend on salinity and, as such, the hydrogen isotopic composition of alkenones is emerging as a palaeosalinity proxy. The relationship between fractionation and salinity has previously only been determined during exponential growth, whilst it is not yet known in which growth phases natural haptophyte populations predominantly exist. We have therefore determined the relationship between the fractionation factor, $\alpha_{alkenones\text{-}water}$, and salinity for C_{37} alkenones produced in different growth phases of batch cultures of the major alkenone-producing coastal haptophytes *Isochrysis galbana* (strain CCMP 1323) and *Chrysotila lamellosa* (strain CCMP 1307) over a range in salinity from ca. 10 to 35. $\alpha_{alkenones\text{-}water}$ was similar in both species, ranging over 0.841–0.900 for *I. galbana* and 0.838–0.865 for *C. lamellosa*. A strong ($0.85 \leq R^2 \leq 0.97$; $p < 0.0001$) relationship between salinity and fractionation factor was observed in both species at all growth phases investigated. This suggests that alkenone δD has the potential to be used as a salinity proxy in neritic areas where haptophyte communities are dominated by these coastal species. However, there was a marked difference in the sensitivity of $\alpha_{alkenones\text{-}water}$ to salinity between different growth phases: in the exponential growth phase of *I. galbana*, $\alpha_{alkenones\text{-}water}$ increased by 0.0019 per salinity unit (S^{-1}), but was less sensitive at 0.0010 S^{-1} and 0.0008 S^{-1} during the stationary and decline phases, respectively. Similarly, in *C. lamellosa* $\alpha_{alkenones\text{-}water}$ increased by 0.0010 S^{-1} in the early stationary phase and by 0.0008 S^{-1} during the late stationary phase. Assuming the shift in sensitivity of $\alpha_{alkenones\text{-}water}$ to salinity observed at the end of exponential growth in *I. galbana* is similar in other alkenone-producing species, the predominant growth phase of natural populations of haptophytes will affect the sensitivity of the alkenone salinity proxy. The proxy is likely to be most sensitive to salinity when alkenones are produced in a state similar to exponential growth.

1 Introduction

One of the important controls of climate in the late Quaternary is ocean circulation (e.g. Broecker et al., 1985), which transports heat and moisture around the globe (Ganachaud and Wunsch, 2000). This circulation depends on, amongst other factors, differences in seawater density, which in turn are partly dependent on salinity. Meanwhile, 86% of evaporation and 78% of precipitation occur over the ocean (Baumgartner and Reichel, 1975), the relative amounts of which affect salinity at the sea surface (e.g. Durack et al., 2012). Therefore, the ability to reconstruct past sea surface salinities is of importance to understand past changes in both ocean dynamics and the hydrological cycle.

Currently, the hydrogen isotopic composition (δD) of C_{37} alkenones is emerging as a potential sea surface salinity proxy. These long-chain alkenones are acetogenic lipids (de Leeuw et al., 1980) produced, in marine environments, by only a few species of haptophyte algae (e.g. Volkman et al., 1980; Marlowe et al., 1984; Volkman et al., 1995) and are well studied because of the application of the alkenone unsaturation indices U^{K}_{37} (Brassell et al., 1986) and $U^{K'}_{37}$ (Prahl and Wakeham, 1987) as palaeotemperature proxies. The alkenone δD salinity proxy exploits two effects: first, a strong correlation between the δD of alkenones and the δD of seawater (Englebrecht and Sachs, 2005), which itself is strongly coupled to salinity (Craig and Gordon, 1965); and second, a correlation of the fractionation factor between water and C_{37} alkenones, $\alpha_{alkenones\text{-}water}$ (α), to salinity (Schouten et al., 2006; M'Boule et al., 2014). These two effects act in concert so that alkenone δD becomes less negative as salinity increases. As such, the δD of alkenones

recovered from sediment cores has been used to estimate changes in past surface salinity, for example, in the Eastern Mediterranean (van der Meer et al., 2007), the Black Sea (van der Meer et al., 2008; Coolen et al., 2013) and the Agulhas region (Kasper et al., 2014).

The reason for this correlation between salinity and fractionation is presently not clear. One hypothesis for the increase in fractionation factor observed with increasing salinity is that at higher salinities water transport across cell membranes is reduced as the cell maintains osmotic potential and that this reduced transport decreases the effective size of the pool of internal cell water from which hydrogen can be fixed (Sachse and Sachs, 2008). It is known that the hydrogen isotopic composition of internal cell water can be considerably different to external water (Kreuzer-Martin et al., 2006). Preferential incorporation of more deuterium (D)-depleted isotopologues of water into the photosynthate via NADPH during photosynthesis (Estep and Hoering, 1981; Yakir and DeNiro, 1990) should leave any remaining intracellular water relatively enriched in deuterium. Therefore, at higher salinities cell water D enrichment is more rapid than at lower salinities. As photosynthesis continues, the signal from this D enriched cell water is then transferred to alkenones, resulting in an apparent increase in α at higher salinities.

Besides salinity, α also varies with other parameters, such as the species producing the alkenones (Schouten et al., 2006; M'Boule et al., 2014), their growth rate (Schouten et al., 2006) and growth phase (Wolhowe et al., 2009). Wolhowe et al. (2009) observed, in batch cultures of the major oceanic alkenone-producing haptophyte species *Emiliania huxleyi* and *Gephyrocapsa oceanica*, a decrease in α after the exponential growth phase. Based on an observed increase in the mass of alkenones per cell after exponential growth (cf., for example, Conte et al., 1998; Epstein et al., 1998; Eltgroth et al., 2005), a possible reason given for this decrease in α was that after the onset of the stationary phase the relative rate of biosynthesis of acetogenic alkenones compared to isoprenoidal structural lipids increases. Because isoprenoidal lipids are more depleted in D relative to acetogenic lipids (Estep and Hoering, 1980; Sessions et al., 1999; Chikaraishi et al., 2009) then — if the rate of NADPH formation is assumed to remain constant in both growth phases — mass balance of the two stable hydrogen isotopes means that as the relative production of alkenones increases their δD must become more negative.

It is not known if and how the growth phases observed in batch culture are applicable to natural continually-growing and occasionally blooming populations of algae, and therefore the predominant growth phase of natural haptophyte populations is unknown. Nevertheless, if natural haptophyte populations are controlled primarily by nutrient limitation then it is more likely that alkenone flux to sediment is derived principally from cells in the stationary or decline phases than if mortality — due to, for example, grazing by zooplankton or infection by viruses — is the controlling factor. Whether or not phytoplankton populations are controlled primarily by nutrient limitation or by grazing or viral lysis is debated (e.g. Banse, 2013 and references cited therein). Meanwhile, the global core-top calibration for the temperature proxy is statistically identical to that observed during the exponential phase of an *E. huxleyi* culture (Müller et al., 1998) but a resemblance in the alkenone and alkenoate composition of surface sediments to those of nutrient stressed haptophyte cells has also been observed (Conte et al., 1998; Prahl et al., 2006). The possibility that natural haptophyte populations exist

at growth phases other than the exponential, together with the effect of growth phase on α, means that, in order to improve the ability of alkenone δD to reconstruct sea surface palaeosalinities in a broad range of environments, the relationship between α and salinity should be determined for growth phases other than the exponential.

M'Boule et al. (2014) determined for the first time the relationship between α and salinity for a coastal haptophyte. The sensitivity of the fractionation factor, α, to salinity (S) in exponential phase *Isochrysis galbana* (where $\alpha = 0.0019\,S + 0.835$; $R^2 = 0.97$, $p < 0.0001$, n = 18; Fig. 1) was similar to that in open ocean haptophytes — extending the potential scope of the alkenone salinity proxy to areas dominated by coastal alkenone-producers as well as those dominated by oceanic species. Here, using batch cultures of the major coastal alkenone-producing haptophytes *I. galbana* and *Chrysotila lamellosa*, we investigate the effects of growth phase on the relationship between α and salinity, and discuss the implications of these effects on the use of alkenone δD for palaeosalinity reconstruction.

2 Materials and methods

2.1 Cultures

Batch cultures of *Isochrysis galbana* (strain CCMP 1323) and *Chrysotila lamellosa* (strain CCMP 1307) were grown in triplicate at salinities of 10.3, 15.3, 20.2, 25.1, 30.2 and 35.5, and 10.2, 15.2, 20.3, 24.9, 30.0 and 35.0, respectively. Waters of different salinities were sterilized by autoclave and enriched with sterile minerals and vitamins to give f/2 medium (Guillard, 1975). Cultures (600 mL) were grown in 1 L Erlenmeyer flasks, sealed by paper stopper, at 15°C under cool white fluorescent lights (Philips Master TL-D 865) providing 60 μmol photons m^{-2} s^{-1} with a light:dark cycle of 16:8 h. Cultures were inoculated to an initial cell density of between 2300–4600 cells mL^{-1} (*I. galbana*; M'Boule, et al., 2014) and 500–1500 cells mL^{-1} (*C. lamellosa*) using stock cultures that had been acclimatized under the above conditions at each salinity for five weeks, during which the culture was transferred to fresh medium five times. After inoculation cell densities were monitored regularly by flow cytometry (Accuri C6) and growth phases were determined from plots of the natural log of cell concentration against incubation time (Appendix A, Fig A1; cell concentrations are displayed in Appendix A, Tables A1 and A2). Cell material, together with water for hydrogen isotope and salinity analyses, was collected from the *I. galbana* cultures after 10 (exponential growth phase; M'Boule et al., 2014), 27 or 28 days (stationary phase) and 69, 75, 83, or 89 days (decline phase; Table 1), and from the *C. lamellosa* cultures after 13 or 14 (early stationary phase) and 35 days (late stationary phase). Biomass was collected following M'Boule et al. (2014). Salinity measurements were determined immediately by conductivity meter (VWR EC300) calibrated to IAPSO standard seawater of salinities 10, 30, 35 and 37.

2.2 Lipid extraction and separation

Cell material was extracted from freeze-dried GF/F filters (Whatman) into 2:1 (v/v) dichloromethane:methanol (4×10 mL; 4×5 min sonication), after the addition of an *n*-nonadecan-10-one (Sigma) internal standard. The extracts were combined and evaporated under vacuum before being dried over sodium sulfate. The total lipid extract was separated using an alumina column into three fractions: apolar (eluted with three column volumes of 9:1 (v/v) hexane/dichloromethane), alkenone (eluted with four column volumes of 1:1 (v/v) hexane/dicholormethane) and polar (eluted with four

column volumes of 1:1 (v/v) dichloromethane/methanol). The alkenone fraction was analysed by gas chromatography (GC) and GC/mass spectrometry (GC/MS) according to Chivall et al. (2014).

2.3 Hydrogen isotope analysis

Water for hydrogen isotope determinations was stored with no headspace in 12 mL exertainers (Labco) in the dark at ~5°C until analysis. δD of culture medium (10 × ~1 μL) was determined by elemental analysis/thermal conversion/isotope ratio monitoring MS (EA/TC/irmMS) using a ThermoQuest Finnigan TC/EA interfaced via a ThermoQuest Finnigan MAT ConFlo III to a ThermoQuest Finnigan Delta^{Plus} XL mass spectrometer as reported by M'Boule et al. (2014). The H_3^+ factor was determined daily and varied from 7.3–7.8 ppm mV^{-1} at < 0.1 ppm mV^{-1} day^{-1}.

Hydrogen isotope analysis of the alkenone fraction was performed by GC/TC/irmMS using an Agilent 7890 GC connected via Thermo GC Isolink and Conflo IV interfaces to a Thermo Delta V mass spectrometer in the same manner as M'Boule et al. (2014). The H_3^+ factor varied from 5.8–6.5 ppm mV^{-1} at not more than 0.1 ppm mV^{-1} day^{-1}. To monitor accuracy, squalane and *n*-triacontane were co-injected with each alkenone sample. δD of co-injected squalane was -172 ± 3‰ (n = 182), which compares well with its EA determined δD of -170 ± 4‰; δD of co-injected *n*-triacontane was -75 ± 3‰ (n = 182; EA determined value = -79 ± 5‰). Alkenone δD was determined as the combined peak of C_{37} alkenones (van der Meer et al., 2013) and were measured in duplicate; values reported are the mean.

2.4 Calculation of alkenone concentration and net rate of production

The mass of C_{37} alkenones recovered per cell (Table 1; Fig. 3a) was calculated as the ratio between the mass of alkenones recovered per mL of culture (Appendix A, Table A3) and, for sampling during the exponential and stationary phases, the cell concentration at the time of sampling; for the decline phase the mean cell concentration during the stationary phase was used. The net rate of alkenone production during the incubation period (Table 1; Fig. 3b) was calculated as the ratio between the mass of alkenones recovered per mL of culture and the integral of a plot of cell concentration against incubation period.

3 Results

Batch cultures of *I. galbana* and *C. lamellosa* were grown over a range of salinities and sampled during different growth phases (Tables 1 and 2). Alkenone distributions and concentrations have been reported elsewhere (Chivall et al., 2014), as has alkenone δD and the α-S relationship for exponential phase *I. galbana* (M'Boule et al., 2014). For *C. lamellosa*, problems with cell counting, probably caused by cell clumping (Green and Course, 1983), made it difficult to calculate growth rates and to identify the transition between growth phases, which meant no sampling occurred during the exponential phase. We have therefore termed the sampling at 13 or 14 days early stationary phase and at 35 days, late stationary phase.

The δD of C_{37} alkenones recovered from the stationary phase of the *I. galbana* cultures ranged from -181 ± 1‰ (S = 10.3) to -124 ± 1‰ (S = 35.8) and, for the decline phase, from -174 ± 2‰ (S = 10.7) to 123 ± 2‰ (S = 37.4; Table 1). Due to its preparation from seawater and ultrapure water of different isotopic compositions the δD of the medium increased linearly with salinity over a range from -30 ± 2 ‰ to +9 ± 2‰ (Table 1). The resulting relationships between the fractionation factor, α, and salinity during the stationary and decline phases can be expressed as $\alpha = 0.0010\ S + 0.833$ ($R^2 = 0.88$, $p < 0.0001$, n = 18) and $\alpha = 0.0008\ S + 0.839$ ($R^2 = 0.95$, $p < 0.0001$, n = 18; both Fig. 1), respectively.

The range in alkenone δD taken from *C. lamellosa* during the early stationary phase was -189 ± 2‰ (S = 10.2) to -131 ± 1‰ (at S = 35.0) and during the late stationary phase was -187 ± 1‰ (S = 10.2) to -134 ± 1‰ (at S = 35.2; Table 2). Again, water δD increased linearly with salinity from -33 ± 2‰ to +5 ± 3‰ (Table 2). The resulting α-S relationship for alkenones recovered during the early stationary phase can be expressed as $\alpha = 0.0010\ S + 0.829$ ($R^2 = 0.97$, $p < 0.0001$, n = 18) and that for the late stationary phase as $\alpha = 0.0008\ S + 0.829$ ($R^2 = 0.85$, $p < 0.0001$, n = 18; Fig. 2).

4 Discussion

4.1 The relationship between hydrogen isotopic fractionation and salinity at different growth phases

The range of the fractionation factor, α, for C_{37} alkenones produced by batch cultures of *I. galbana* across all growth phases was 0.841–0.900. This is of similar magnitude to the estimate of $\alpha_{C31alkadiene\text{-}water} = 0.887$ for a culture of *I. galbana* obtained by Sessions et al. (1999). As discussed elsewhere (M'Boule et al., 2014), the fractionation observed in *I. galbana* was less than that observed in the major alkenone-producing oceanic haptophytes *E. huxleyi* ($0.760 \leq \alpha \leq 0.822$; Schouten et al., 2006; D'Andrea et al., 2007; Wolhowe et al., 2009; M' Boule et al., 2014) and *G. oceanica* ($0.737 \leq \alpha \leq 0.809$; Schouten et al., 2006; Wolhowe et al., 2009). Fractionation in *C. lamellosa* ($0.838 \leq \alpha \leq 0.865$) was similar to *I. galbana*. This suggests that hydrogen fractionation in coastal haptophytes is in general less than that of open ocean haptophytes, perhaps because of differing strategies for maintaining homeostasis in relationship to salinity changes in coastal and oceanic species (M'Boule et al., 2014).

During exponential growth α for *I. galbana* increases by 0.0019 per unit increase in salinity (S^{-1}; M'Boule et al., 2014), which is less than that observed in *E. huxleyi* ($0.0021 \leq S^{-1} \leq 0.0033$; Schouten et al., 2006; M'Boule et al., 2014) and *G. oceanica* (0.0030 S^{-1}; Schouten et al., 2006). The results presented here clearly show that the sensitivity of α to salinity not only depends on species but also on growth phase. During the stationary and decline phases of *I. galbana* the sensitivity of α to salinity was approximately halved to 0.0010 S^{-1} and 0.0008 S^{-1}, respectively (Fig. 1). The difference between the gradients of the slopes of the α-S relationship in the stationary and decline phases is not significant (linear regression analysis; $p = 0.06$) whilst the difference between the equations of the slopes is weakly significant (analysis of covariance; $p = 0.04$). This suggests that the change in cell physiology or biochemistry affecting the α-S relationship mainly occurs at the end of exponential growth and the cell then remains in a similar state until cell death.

Similarly, for *C. lamellosa*, α increased by 0.0010 S^{-1} during the early stationary phase and by 0.0008 S^{-1} during the late stationary phase. The gradients of the slopes of the α-S relationships at both sampling times for *C. lamellosa* are not significantly different from each other (linear regression analysis; $p = 0.08$; Fig. 2). Meanwhile, the gradients of the slopes of the same plot for early stationary phase *C. lamellosa* and stationary phase *I. galbana* are the same (linear regression analysis: $p = 0.21$) and at all growth phases for both species, the intercepts of the α-S relationships are ca. 0.83. Altogether, this suggests that a change in growth phase affects mainly the slope of the α-S relationship and not the intercept and that the changes in fractionation of hydrogen with salinity and growth phase during the biosynthesis of alkenones in both these coastal species are caused by similar processes. Furthermore, at a salinity of 35, α for *I. galbana* decreases by 0.026–0.030 between the exponential and stationary phases which is comparable to the magnitude of the same change observed by Wolhowe et al. (2009) in cultures of *E. huxleyi* (0.023–0.030) and *G. oceanica* (0.022–0.033; both species grown at salinity ~32) and suggests that a similar mechanism is causing the shift with growth phase in the open ocean species as well.

4.2 The relationship between hydrogen isotopic fractionation and alkenone distribution

The change in hydrogen isotopic composition of the C_{37} alkenones between growth phases may be related to a change in distribution of alkenones since the hydrogen isotopic composition of diunsaturated and triunsaturated C_{37} alkenones from the same source can differ by several tens of per mil (D'Andrea et al., 2007; Schwab and Sachs, 2009; Wolhowe et al., 2009; van der Meer et al., 2013). These differences appear to be related to the relative abundance of individual alkenones (van der Meer et al., 2013; Nelson and Sachs, 2014), probably because the $C_{37:3}$ alkenone is likely biosynthesised by desaturation of $C_{37:2}$ (Rontani et al, 2006). The C_{37} alkenone distributions in *I. galbana* and *C. lamellosa* varied with both salinity and growth phase: $U^{K'}_{37}$ decreased in later growth phases and the relative abundance of $C_{37:4}$ ($\%C_{37:4}$) tended to increase with salinity (Table 1; Chivall et al., 2014). While δD of individual alkenones was not determined in this study, it has been calculated previously that a similar change in $U^{K'}_{37}$ at the end of exponential growth in an *E. huxleyi* culture did not alter α by more than instrumental error (Wolhowe et al., 2009). Furthermore, there were significant differences in alkenone distribution between the stationary and decline phases of *I. galbana* and between the early and late stationary phases of *C. lamellosa* (Chivall et al., 2014) which were not reflected in the hydrogen isotopic composition of the alkenones. Therefore, as with *E. huxleyi* (Wolhowe et al., 2009), it appears that the cause of the change in the α-S relationship is a change in biosynthetic fractionation rather than alkenone distribution.

Despite the above, we do observe some correlation between α and $\%C_{37:4}$ or $U^{K'}_{37}$ within each growth phase. This correlation in nearly all cases only arises because of a relatively weak correlation between alkenone distribution and salinity (Chivall et al., 2014) and the strong relationship observed between α and salinity. Multiple linear regression analysis with salinity and either $\%C_{37:4}$ or $U^{K'}_{37}$ as independent variables shows that in *I. galbana* there is no significant dependence of α on either $\%C_{37:4}$ ($0.19 \leq p \leq 0.89$) or $U^{K'}_{37}$ ($0.14 \leq p \leq 0.98$). For *C. lamellosa* the same analysis shows no significant contribution to α from $\%C_{37:4}$ ($0.09 \leq p \leq 0.93$) or, in the early stationary phase, from $U^{K'}_{37}$ ($p = 0.46$). However, in the late stationary phase there is a weak dependence of α on $U^{K'}_{37}$ ($p = 0.02$; including

$U^{K'}_{37}$ in the linear regression model increases R^2 to 0.89, compared to $R^2 = 0.84$ when α is modelled against salinity as the sole independent variable). Moreover, alkenone δD typically becomes more negative with increasing unsaturation (D'Andrea et al., 2007; Schwab and Sachs, 2009; Wolhowe et al., 2009; van der Meer et al., 2013) and so the observed increase of $\%C_{37:4}$ with salinity would be expected to result in a decrease in α rather than the observed increase. With the caveat that the effect of alkenone distribution upon α was not explicitly tested, it appears that in these cultures alkenone distribution has little effect on δD of the combined C_{37} alkenones.

4.3 Possible causes for the effect of growth phase on α

A previously proposed mechanism (Wolhowe et al., 2009) for the change in biosynthetic fractionation at the end of exponential growth is based on the relative rate of production of acetogenic and isoprenoidal lipids. If the production of relatively D-depleted isoprenoidal structural components decreases after exponential growth due to a reduction in cell division, but NADPH production continues into the stationary phase, then excess hydride is likely to be used for the synthesis of alkenones. Mass balance suggests that the relative increase in production of acetogenic alkenones after exponential growth will cause them to become further D-depleted. This hypothesis may be supported by the typically observed increase in the mass of alkenones per cell after exponential growth (e.g. Conte et al., 1998; Epstein et al., 1998; Eltgroth et al., 2005). Relative rates of production of acetogenic and isoprenoidal lipids were not measured in this study, however an interesting observation is that although the mass of C_{37} alkenones per cell increases after the exponential phase (Table 1; Fig. 3a; Chivall et al., 2014) the net rate of production of alkenones per cell actually falls after exponential growth (Table 1; Fig. 3b).

An alternative explanation for the change in biosynthetic fractionation at the onset of the stationary phase is based on internal cell water. Since ^1H is preferentially used in the reduction of $NADP^+$ to NADPH (Estep and Hoering, 1981; Yakir and DeNiro, 1990), the increase in α with increasing salinity observed in haptophytes could be due to a reduction in water transport across the cell membrane at higher salinities, resulting in a greater D enrichment of internal cell water than at lower salinities (Sachse and Sachs, 2008). Nutrient limitation can decrease the photosynthetic efficiency of haptophytes (Herrig and Falkowski, 1989) and, because the rate of NADPH production is linked to the rate of photosynthesis, it is likely that the rate of hydrogen incorporation into NADPH from cell water also falls during conditions of nutrient limitation, such as after the exponential growth phase. This is consistent with the decrease in the net rate of alkenone production in *I. galbana* after exponential growth (Fig. 3b). If the rate of water transport across the cell membrane remains constant while the rate of incorporation of hydrogen into NADPH falls, then the effective size of the internal water pool, relative to the rate of hydrogen incorporation into NADPH, will be larger. This would lead to a smaller D enrichment of cell water at a given salinity and would explain both the apparent decrease in α observed at a given salinity and the decreased sensitivity of α to changing salinity after exponential growth. Alternative explanations that would cause the same change in cell water D enrichment are that the integrity of the cell membrane decreases after exponential growth, or that cell volume increases after exponential growth (observed in *E. huxleyi*; Franklin et al., 2012). Determinations of the δD of internal cell water of these haptophytes at different salinities and growth phases would need to be made in order to test this hypothesis.

4.4 Implications for the alkenone palaeosalinity proxy

There is a strong ($0.85 \leq R^2 \leq 0.97$; $p < 0.0001$) α-S relationship in both coastal alkenone producing species at all growth phases studied, suggesting that alkenone δD has potential to be used as a salinity proxy in coastal as well as oceanic regions. Hydrogen isotope fractionation in both species is similar, as are the relationships between α and salinity in the stationary phase. If *C. lamellosa* behaves in a similar way to *I. galbana* during exponential growth, then it is likely that an alkenone δD salinity proxy will not be highly sensitive to a change in composition of coastal alkenone producing species. However, as noted by M'Boule et al. (2014), there is a significant difference in the magnitude of isotope fractionation between the coastal haptophytes *I. galbana* and *C. lamellosa* and the major oceanic alkenone producing haptophytes *E. huxleyi* and *G. oceanica*. Because of this, the species composition of alkenone producing haptophytes must be considered when applying alkenone δD as a salinity proxy in transitions from open marine to increasingly coastal environments.

The general lack of dependence of α upon alkenone distribution in these cultures supports the argument that δD of a combined C_{37} alkenones peak can be used for salinity reconstructions (in agreement with van der Meer et al., 2013). However, the effect of alkenone distribution on α has not yet been explicitly tested. Meanwhile, multiple linear regression analysis of the Schouten et al. (2006) *G. oceanica* data (available at http://dx.doi.org/10.1594/PANGAEA.832017), shows that α is dependent on both salinity and $U^{K'}_{37}$ (both $p < 0.001$). Regressing α for *G. oceanica* against both salinity and $U^{K'}_{37}$ increases R^2 to 0.97 compared to $R^2 = 0.61$ when α is regressed against salinity alone. If there is a general effect of alkenone distribution on α then the likely consistent relationship between $\alpha_{C37:3\text{-}C37:2}$ and $U^{K'}_{37}$ (van der Meer et al., 2013; Nelson and Sachs, 2014) could be used to correct for variations in $U^{K'}_{37}$ without having to know the isotopic composition of the individual alkenones. This approach may be favoured for palaeoenvironmental studies, where a high sample throughput and low abundance measurements are required.

The effect of growth phase may complicate salinity reconstructions. In cultures of *I. galbana*, the sensitivity of α to salinity was greater in the exponential growth phase than in the stationary or decline phases. Based on the decrease in α at the onset of the stationary phase observed in batch cultures of *E. huxleyi* and *G. oceanica* (Wolhowe et al., 2009) and the *C. lamellosa* data presented here, it seems likely that a similar relationship also exists for these three other major alkenone producers. Assuming this to be the case — and that the concept of growth phases is applicable to natural populations of alkenone-producing haptophytes — it will be crucial to know in which growth phase are the alkenones produced that end up in the geological record because the sensitivity of the alkenone palaeosalinity proxy will decrease if a large proportion of these alkenones are produced in growth states similar to those after exponential growth. However, the lower sensitivity of α to salinity observed in alkenones from the later growth phases of these cultures does not explain the low sensitivities observed in alkenones recovered from an estuarine (Schwab and Sachs, 2011) and lacustrine environments (Nelson and Sachs, 2014). A further complication may be that a change in nutrient availability accompanying a shift in salinity may cause a change of nutrient stress or growth phase in an alkenone-producing population or a change in the population itself, both of which are likely to affect alkenone δD. Because the predominant growth phase of natural populations of alkenone-producing haptophytes

is unknown, a core-top calibration of the relationship between the fractionation factor, α, and salinity should be performed to understand the effect of growth phase on the hydrogen isotopic composition of alkenones in nature and, thereby, improve alkenone δD as a palaeosalinity proxy.

5 Conclusions

The hydrogen isotopic composition of alkenones recovered from batch cultures of *I. galbana* and *C. lamellosa* is strongly dependent on salinity: a strong relationship between the fractionation factor, α, and salinity is observed in both species in all growth phases studied. However, the hydrogen isotopic composition of alkenones in batch cultures of *I. galbana* is also strongly dependent on growth phase: the sensitivity of α to changes in salinity is reduced after the exponential growth phase. A similar effect appears likely in the three other main alkenone producing species. The predominant growth phase of natural populations of haptophytes will therefore affect the sensitivity of the alkenone palaeosalinity proxy.

Acknowledgments

We thank A. A. M. Noordeloos and the Department of Biological Oceanography at NIOZ for assistance with algal culturing. A. L. Sessions and three anonymous reviewers are thanked for their comments on the manuscript. This project was funded by the Netherlands Organization for Scientific Research (NWO) through Project ALW818.01.022. NWO is also acknowledged for funding M. T. J. van der Meer (VIDI).

Associate editor: Alex L. Sessions

References

Banse K. (2013) Reflections about chance in my career, and on the top-down regulated world. *Annu. Rev. Mar. Sci.* **5**, 1-19.

Baumgartner A. and Reichel E. (1975) *World Water Balance: Mean Annual Global, Continental and Maritime Precipitation, Evaporation and Runoff*. Elsevier, Amsterdam.

Brassell S. C., Brereton R. G., Eglinton G., Grimalt J., Liebezeit G., Marlowe I. T., Pflaumann U. and Sarnthein M. (1986) Paleoclimatic signals recognized by chemometric treatment of molecular stratigraphic data. *Org. Geochem.* **10**, 649-660.

Broecker W. S., Peteet D. M. and Rind D. (1985) Does the ocean-atmosphere system have more than one stable mode of operation? *Nature* **315**, 21-26.

Chikaraishi Y., Tanaka R., Tanaka A. and Ohkouchi N. (2009) Fractionation of hydrogen isotopes during phytol biosynthesis. *Org. Geochem.* **40**, 569-573.

Chivall D., M'Boule D., Sinke-Schoen D., Sinninghe Damsté J S., Schouten, S. and van der Meer, M. T. J. (2014) Impact of salinity and growth phase on alkenone distributions of coastal haptophytes. *Org. Geochem.* **67**, 31-34.

Conte M. H., Thompson A., Lesley D. and Harris R. P. (1998) Genetic and physiological influences on the alkenone/alkenoate versus growth temperature relationship in *Emiliania huxleyi* and *Gephyrocapsa oceanica*. *Geochim. Cosmochim. Acta* **62**, 51-68.

Coolen M. J. L., Orsi W. D., Balkema C., Quince C., Harris K., Sylva S. P., Filipova-Marinova M. and Giosan L. (2013) Evolution of the plankton paleome in the Black Sea from the Deglacial to Anthropocene. *Proc. Natl. Acad. Sci. U.S.A.* **110**, 8609-8614.

Craig H. and Gordon L. I. (1965) Deuterium and oxygen 18 variations in the ocean and marine atmosphere. In *Proceedings of a Conference on Stable Isotopes in Oceanographic Studies and Paleotemperatures* (ed. E. Tongiogi). V. Lishi e F. Pisa, Spoleto, Italy. pp. 9-130.

D'Andrea W. J., Liu Z. H., Alexandre M. D., Wattley S., Herbert T. D. and Huang Y. S. (2007) An efficient method for isolating individual long-chain alkenones for compound-specific hydrogen isotope analysis. *Anal. Chem.* **79**, 3430-3435.

de Leeuw J. W., van der Meer F. W., Rijpstra W. I. C. and Schenk P. A. (1980) On the occurrence and structural identification of long chain unsaturated ketones and hydrocarbons in sediments. In *Advances in Organic Geochemistry 1979* (eds. A. G. Douglas and J. R. Maxwell). Pergamon, Oxford. pp. 211-217.

Durack P. J., Wijffels S. E. and Matear R. J. (2012) Ocean salinities reveal strong global water cycle intensification during 1950 to 2000. *Science* **336**, 455-458.

Eltgroth M. L., Watwood R. L. and Wolfe G. V. (2005) Production and cellular localization of neutral long-chain lipids in the haptophyte algae *Isochrysis galbana* and *Emiliania huxleyi*. *J. Phycol.* **41**, 1000-1009.

Englebrecht A. C. and Sachs J. P. (2005) Determination of sediment provenance at drift sites using hydrogen isotopes and unsaturation ratios in alkenones. *Geochim. Cosmochim. Acta* **69**, 4253-4265.

Epstein B. L., D'Hondt S., Quinn J. G., Zhang J. P. and Hargraves P. E. (1998) An effect of dissolved nutrient concentrations on alkenone-based temperature estimates. *Paleoceanography* **13**, 122-126.

Estep M. F. and Hoering T. C. (1980) Biogeochemistry of the stable hydrogen isotopes. *Geochim. Cosmochim. Acta* **44**, 1197-1206.

Estep M. F. and Hoering T. C. (1981) Stable hydrogen isotope fractionations during autotrophic and mixotrophic growth of microalgae. *Plant Physiol.* **67**, 474-477.

Franklin D. J., Airs R. L., Fernandes M., Bell T. G., Bongaerts R. J., Berges J. A. and Malin G. (2012) Identification of senescence and death in *Emiliania huxleyi* and *Thalassiosira pseudonana*: Cell staining, chlorophyll alterations, and dimethylsulfoniopropionate (DMSP) metabolism. *Limnol. Oceanogr.* **57**, 305-317.

Ganachaud A. and Wunsch C. (2000) Improved estimates of global ocean circulation, heat transport and mixing from hydrographic data. *Nature* **408**, 453-457.

Green J. C. and Course P. A. (1983) Extracellular calcification in *Chrysotila lamellosa* (Prymnesiophyceae). *Brit. Phycol. J.* **18**, 367-382.

Guillard R. R. L. (1975) Culture of phytoplankton for feeding marine invertebrates. In *Culture of Marine Invertebrate Animals* (eds. W. L. Smith and M. H. Chanley). Plenum Press, New York. pp. 26-60.

Herrig R. and Falkowski P. G. (1989) Nitrogen limitation in *Isochrysis galbana* (Haptophyceae). 1. Photosynthetic energy conversion and growth efficiencies. *J. Phycol.* **25**, 462-471.

Kasper S., van der Meer M. T. J., Mets A., Zahn R., Sinninghe Damsté J. S., and Schouten S. (2014) Salinity changes in the Agulhas leakage area recorded by stable hydrogen isotopes of C_{37} alkenones during Termination I and II, *Clim. Past* **10**, 251-260.

Kreuzer-Martin H. W., Lott M. J., Ehleringer J. R. and Hegg E. L. (2006) Metabolic processes account for the majority of the intracellular water in log-phase *Escherichia coli* cells as revealed by hydrogen isotopes. *Biochemistry* **45**, 13622-13630.

Marlowe I. T., Green J. C., Neal A. C., Brassell S. C., Eglinton G. and Course P. A. (1984) Long-chain (*n*-C37-C39) alkenones in the Prymnesiophyceae. Distribution of alkenones and other lipids and their taxonomic significance. *Brit. Phycol. J.* **19**, 203-216.

M'Boule D., Chivall D., Sinke-Schoen D., Sinninghe Damsté J. S., Schouten S. and van der Meer, M. T. J. (2014) Salinity dependent hydrogen isotope fractionation in alkenones produced by open ocean and coastal haprophyte algae. *Geochim. Cosmochim. Acta* **130**, 126-135.

Müller P. J., Kirst G., Ruhland G., von Storch I. and Rosell-Mele A. (1998) Calibration of the alkenone paleotemperature index $U^{K'}_{37}$ based on core-tops from the eastern South Atlantic and the global ocean (60°N–60°S). *Geochim. Cosmochim. Acta* **62**, 1757-1772.

Nelson D. B. and Sachs J. P. (2014) The influence of salinity on D/H fractionation in alkenones from saline and hypersaline lakes in continental North America. *Org. Geochem.* **66**, 38-47.

Prahl F. G. and Wakeham S. G. (1987) Calibration of unsaturation patterns in long-chain ketone compositions for paleotemperature assessment. *Nature* **330**, 367-369.

Prahl F. G., Mix A. C. and Sparrow M. A. (2006) Alkenone paleothermometry: Biological lessons from marine sediment records off western South America. *Geochim. Cosmochim. Acta* **70**, 101-117.

Rontani J. F., Prahl F. G. and Volkman J. K. (2006) Re-examination of the double bond positions in alkenones and derivatives: Biosynthetic implications. *J. Phycol.* **42**, 800-813.

Sachse D. and Sachs J. P. (2008) Inverse relationship between D/H fractionation in cyanobacterial lipids and salinity in Christmas Island saline ponds. *Geochim. Cosmochim. Acta* **72**, 793-806.

Schouten S., Ossebaar J., Schreiber K., Kienhuis M. V. M., Langer G., Benthien A. and Bijma J. (2006) The effect of temperature, salinity and growth rate on the stable hydrogen isotopic composition of long chain alkenones produced by *Emiliania huxleyi* and *Gephyrocapsa oceanica*. *Biogeosciences* **3**, 113-119.

Schwab V. F. and Sachs J. P. (2009) The measurement of D/H ratio in alkenones and their isotopic heterogeneity. *Org. Geochem.* **40**, 111-118.

Schwab V. F. and Sachs J. P. (2011) Hydrogen isotopes in individual alkenones from the Chesapeake Bay estuary. *Geochim. Cosmochim. Acta* **75**, 7552-7565.

Sessions A. L., Burgoyne T. W., Schimmelmann A. and Hayes J. M. (1999) Fractionation of hydrogen isotopes in lipid biosynthesis. *Org. Geochem.* **30**, 1193-1200.

van der Meer M. T. J., Baas M., Rijpstra W. I. C., Marino G., Rohling E. J., Sinninghe Damsté J. S. and Schouten S. (2007) Hydrogen isotopic compositions of long-chain alkenones record freshwater flooding of the Eastern Mediterranean at the onset of sapropel deposition. *Earth Planet. Sci. Lett.* **262**, 594-600.

van der Meer M. T. J., Sangiorgi F., Baas M., Brinkhuis H., Sinninghe Damsté J. S. and Schouten S. (2008) Molecular isotopic and dinoflagellate evidence for Late Holocene freshening of the Black Sea. *Earth Planet. Sci. Lett.* **267**, 426-434.

van der Meer M. T. J., Benthien A., Bijma J., Schouten S. and Damste J. S. S. (2013) Alkenone distribution impacts the hydrogen isotopic composition of the $C_{37:2}$ and $C_{37:3}$ alkan-2-ones in *Emiliania huxleyi*. *Geochim. Cosmochim. Acta* **111**, 162-166.

Volkman J. K., Eglinton G., Corner E. D. S. and Sargent J. R. (1980) Novel unsaturated straight-chain C_{37}–C_{39} methyl and ethyl ketones in marine sediments and a coccolithophore *Emiliania huxleyi*. In *Advances in Organic Geochemistry, 1979* (eds. A. G. Douglas and J. R. Maxwell). Pergamon Press, Oxford. pp. 219-227.

Volkman J. K., Barrett S. M., Blackburn S. I. and Sikes E. L. (1995) Alkenones in *Gephyrocapsa oceanica*: Implications for studies of paleoclimate. *Geochim. Cosmochim. Acta* **59**, 513-520.

Wolhowe M. D., Prahl F. G., Probert I. and Maldonado M. (2009) Growth phase dependent hydrogen isotopic fractionation in alkenone-producing haptophytes. *Biogeosciences* **6**, 1681-1694.

Yakir D. and Deniro M. J. (1990) Oxygen and hydrogen isotope fractionation during cellulose metabolism in *Lemma gibba* L. *Plant Physiol.* **93**, 325-332.

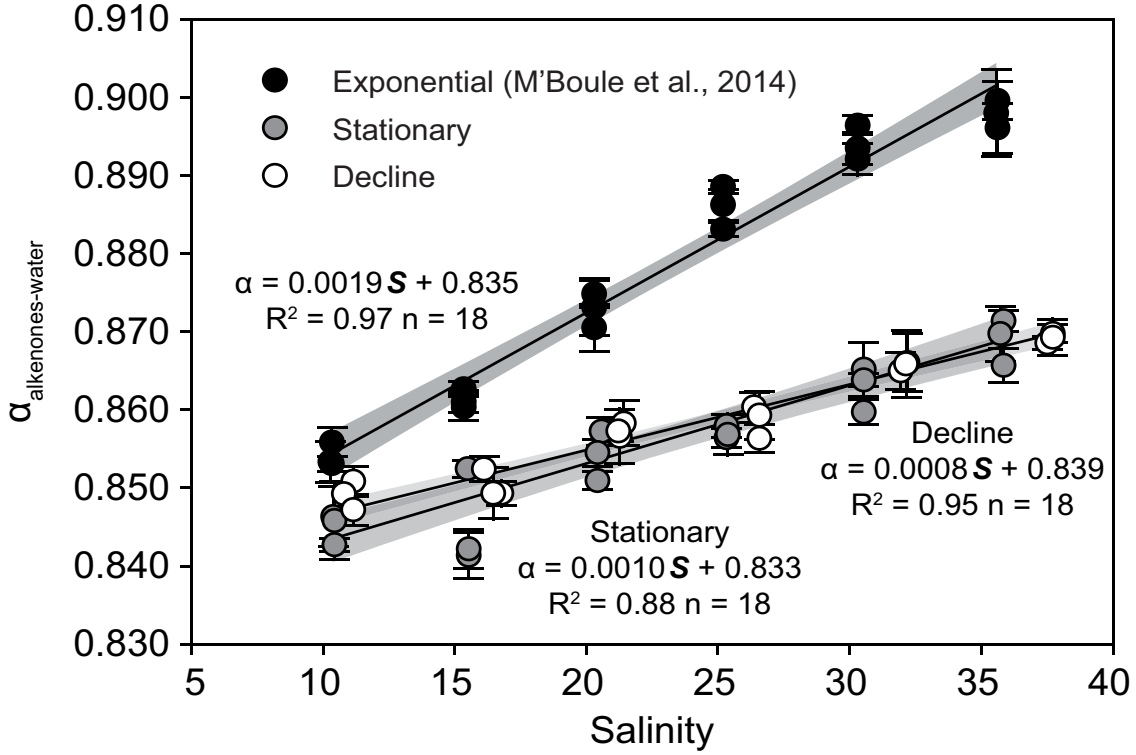

Figure 1. Plot of the fractionation factor, $\alpha_{alkenones\text{-}water}$, against salinity for C_{37} alkenones recovered from batch cultures of *Isochrysis galbana*. Shaded areas are the 95% confidence intervals for the lines of regression. Data from the exponential growth phase are from M'Boule et al. (2014).

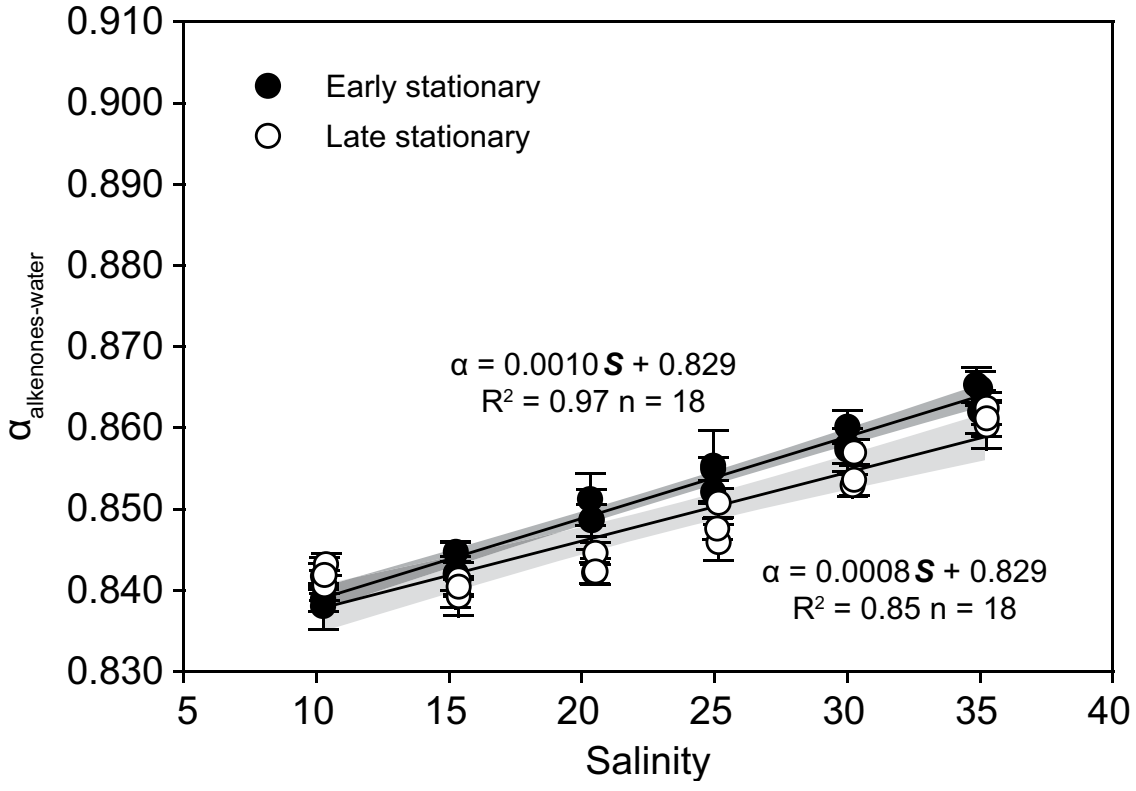

Figure 2. Plot of the fractionation factor, $\alpha_{alkenones\text{-}water}$, against salinity for C_{37} alkenones recovered from batch cultures of *Chrysotila lamellosa*. Shaded areas are the 95% confidence intervals for the lines of regression.

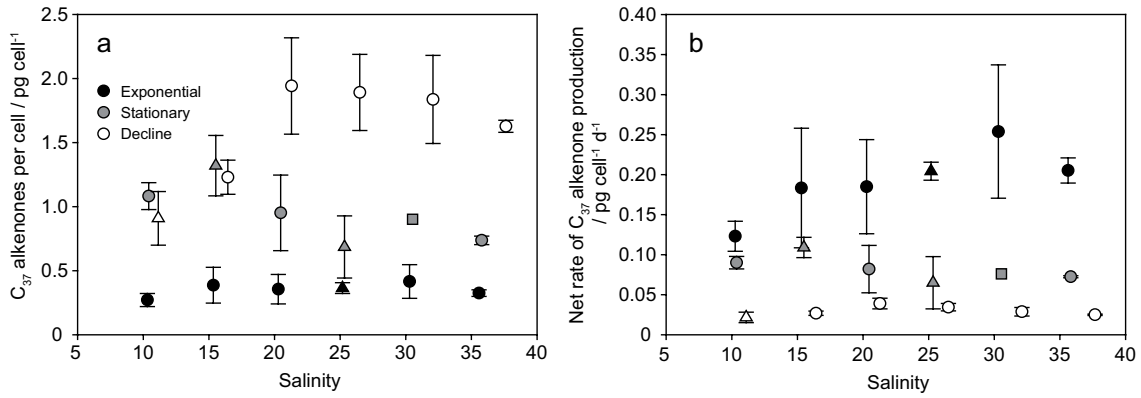

Figure 3. a) Alkenone concentration (from Chivall et al., 2014) and **b)** net rate of alkenone production for batch cultures of *Isochrysis galbana*. Net rate of alkenone production is for the entire incubation period and is not growth phase specific. Circles are the mean ± 1σ of triplicate cultures; triangles are the mean of two cultures (the error is the range); and squares are data from a single culture.

Table 1

Salinity, incubation time, growth rate, $\delta D_{alkenones}$, δD_{water}, $\alpha_{alkenones\text{-}water}$, $U^{K'}_{37}$, $\%_{C37:4}$, alkenone concentration and net rate of alkenone production for batch cultures of *Isochrysis galbana* grown at 15°C. δD_{water} and salinity values are the mean of measurements taken at the start of the culture and at the time of sampling. Errors in $\delta D_{alkenones}$ are the range between duplicate measurements unless stated. Errors in δD_{water} are propagated from the standard deviation of at least ten replicate injections. Net rate of alkenone production is for the entire incubation period and is not growth phase specific. Exponential phase data are taken from M'Boule et al. (2014); $U^{K'}_{37}$, %C37:4 and alkenone concentration data are taken from Chivall et al. (2014).

Salinity	Incubation time	Growth rate	$\delta D_{C37alkenones}$	δD_{water}	$\alpha_{alkenones\text{-}water}$	$U^{K'}_{37}$	$\%C_{37:4}$	C_{37} alkenone concentration	Net rate of C_{37} alkenone production
	(d)	(d^{-1})	(‰)	(‰)				(pg cell^{-1})	(pg cell^{-1} day^{-1})
10.3	10	0.63	-172 ± 1	-29 ± 1	0.853 ± 0.001	0.12	6.3	0.24	0.11
10.2	10	0.63	-172 ± 2[a]	-30 ± 1	0.853 ± 0.003	0.12	6.7	0.33	0.15
10.3	10	0.62	-170 ± 1	-30 ± 2	0.856 ± 0.002	0.11	7.2	0.24	0.11
15.3	10	0.58	-158 ± 1[a]	-22 ± 1	0.861 ± 0.001	0.12	6.0	0.27	0.13
15.3	10	0.61	-157 ± 1	-22 ± 1	0.863 ± 0.001	0.11	7.3	0.35	0.16
15.3	10	0.61	-158 ± 1	-22 ± 1	0.860 ± 0.002	0.11	4.4	0.54	0.27
20.3	10	0.63	-142 ± 3	-17 ± 2	0.873 ± 0.004	0.11	5.7	0.26	0.13
20.3	10	0.65	-140 ± 1	-17 ± 2	0.875 ± 0.002	0.11	6.1	0.33	0.18
20.3	10	0.65	-144 ± 3	-16 ± 2	0.871 ± 0.003	0.12	5.5	0.48	0.25
25.2	10	0.61	-122 ± 1	-9 ± 2	0.886 ± 0.002	0.11	6.1	0.39	0.21
25.2	10	0.63	-126 ± 1	-11 ± 1	0.883 ± 0.001	0.12	7.4	n.d.	n.d.
25.2	10	0.64	-121 ± 1	-10 ± 1	0.889 ± 0.001	0.11	7.9	0.34	0.20
30.3	10	0.63	-111 ± 1	-3 ± 2	0.892 ± 0.002	0.10	8.4	0.52	0.32
30.3	10	0.63	-106 ± 1	-3 ± 1	0.896 ± 0.001	0.12	8.6	0.46	0.29
30.3	10	0.63	-109 ± 2	-2 ± 1	0.893 ± 0.002	0.11	9.2	0.27	0.16
35.6	10	0.62	-97 ± 2	+4 ± 2	0.900 ± 0.002	0.11	12	0.33	0.22
35.6	10	0.60	-99 ± 3[a]	+5 ± 1	0.896 ± 0.003	0.12	11	0.35	0.21
35.5	10	0.63	-98 ± 5[a]	+5 ± 1	0.898 ± 0.006	0.09	12	0.30	0.19

continued...

Table 1 (continued)

Salinity	Incubation time	Growth rate	$\delta D_{C37alkenones}$	δD_{water}	$\alpha_{alkenones\text{-}water}$	$U^{K'}_{37}$	$\%C_{37:4}$	C_{37} alkenone concentration	Net rate of C_{37} alkenone production
	(d)	(d^{-1})	(‰)	(‰)				(pg $cell^{-1}$)	(pg $cell^{-1}$ day^{-1})
10.4	28	n.d.	-177 ± 4[a]	-27 ± 1	0.846 ± 0.004	0.08	5.3	0.97	0.08
10.3	28	n.d.	-181 ± 1	-28 ± 1	0.843 ± 0.001	0.07	5.3	1.1	0.10
10.3	28	n.d.	-177 ± 5	-27 ± 1	0.846 ± 0.005	0.07	5.6	1.2	0.09
15.3	28	n.d.	-175 ± 2	-21 ± 1	0.842 ± 0.003	0.06	5.2	1.4	0.12
15.3	28	n.d.	-176 ± 3	-21 ± 1	0.841 ± 0.003	0.07	5.4	1.2	0.10
15.5	28	n.d.	-167 ± 1	-22 ± 1	0.852 ± 0.001	0.07	5.2	n.d.	n.d.
20.4	27	n.d.	-158 ± 2	-15 ± 1	0.855 ± 0.002	0.07	5.3	1.2	0.11
20.5	27	n.d.	-156 ± 1	-16 ± 2	0.857 ± 0.002	0.08	3.5	0.63	0.05
20.4	27	n.d.	-162 ± 1	-15 ± 1	0.851 ± 0.001	0.08	4.4	1.0	0.09
25.3	28	n.d.	-152 ± 1	-10 ± 1	0.856 ± 0.001	0.07	5.4	n.d.	n.d.
25.3	28	n.d.	-150 ± 1	-9 ± 1	0.858 ± 0.001	0.09	2.8	0.56	0.05
25.3	28	n.d.	-151 ± 2	-9 ± 1	0.857 ± 0.003	0.07	4.4	0.81	0.08
30.5	28	n.d.	-138 ± 1	-2 ± 1	0.864 ± 0.001	0.08	6.0	n.d.	n.d.
30.5	28	n.d.	-136 ± 3[a]	-2 ± 1	0.865 ± 0.003	0.07	6.3	n.d.	n.d.
30.5	28	n.d.	-142 ± 1	-2 ± 1	0.860 ± 0.002	0.08	4.9	0.90	0.08
35.8	27	n.d.	-124 ± 1	+5 ± 1	0.871 ± 0.001	0.07	5.2	0.70	0.07
35.8	27	n.d.	-128 ± 2	+7 ±1	0.866 ± 0.002	0.07	6.0	0.76	0.07
35.7	27	n.d.	-126 ± 3	+5 ± 1	0.870 ± 0.004	0.08	6.0	0.76	0.07
10.7	69	n.d.	-171 ± 1	-24 ± 1	0.849 ± 0.002	0.03	6.0	n.d.	n.d.
10.7	69	n.d.	-174 ± 2	-25 ± 1	0.847 ± 0.002	0.03	5.6	1.0	0.03
10.7	69	n.d.	-172 ± 2	-26 ± 1	0.851 ± 0.002	0.03	5.6	0.81	0.02
16.0	69	n.d.	-167 ± 1	-19 ± 2	0.849 ± 0.002	0.03	5.7	1.4	0.03
15.9	69	n.d.	-166 ± 3	-18 ± 2	0.849 ± 0.003	0.03	5.6	1.1	0.02
15.9	69	n.d.	-163 ± 1	-18 ± 1	0.852 ± 0.002	0.03	5.1	1.3	0.03
21.1	75	n.d.	-155 ± 3	-14 ± 2	0.857 ± 0.004	0.03	6.1	1.9	0.04
21.1	75	n.d.	-153 ± 2	-13 ± 2	0.858 ± 0.003	0.03	6.0	1.6	0.03
21.0	75	n.d.	-154 ± 1	-14 ± 1	0.857 ± 0.002	0.03	5.7	2.3	0.05
26.4	83	n.d.	-145 ± 3	-5 ± 2	0.859 ± 0.003	0.02	7.2	2.2	0.04
26.2	83	n.d.	-146 ± 1	-7 ± 2	0.860 ± 0.002	0.03	7.1	1.8	0.03
26.3	83	n.d.	-147 ± 1	-4 ± 2	0.856 ± 0.002	0.03	6.7	1.7	0.03
31.8	89	n.d.	-133 ± 4	+2 ± 2	0.866 ± 0.004	0.02	9.6	2.1	0.03
31.9	89	n.d.	-133 ± 3	+1 ± 2	0.866 ± 0.004	0.02	9.6	1.9	0.03
31.6	89	n.d.	-133 ± 1	+2 ± 3	0.865 ± 0.002	0.02	8.8	1.5	0.02
37.4	89	n.d.	-123 ± 2	+9 ± 2	0.869 ± 0.003	0.02	11	1.6	0.03
37.4	89	n.d.	-123 ± 1	+8 ± 1	0.870 ± 0.001	0.02	10	1.6	0.03
37.3	89	n.d.	-123 ± 1	+9 ± 1	0.869 ± 0.001	0.02	10	1.7	0.03

[a] Mean of triplicate measurement ± 1 standard deviation; n.d. = not determined.

Table 2

Salinity, incubation time, $\delta D_{alkenones}$, δD_{water}, $\alpha_{alkenones\text{-}water}$, $U^{K'}_{37}$ and $\%C_{37:4}$ for batch cultures of *Chrysotila lamellosa* grown at 15°C. Reported errors are as for Table 1. $U^{K'}_{37}$ and $\%C_{37:4}$ data are taken from Chivall et al. (2014).

Salinity	Incubation time (d)	$\delta D_{C37alkenones}$ (‰)	δD_{water} (‰)	$\alpha_{alkenones\text{-}water}$	$U^{K'}_{37}$	$\%C_{37:4}$
10.2	14	-189 ± 2	-32 ± 2	0.838 ± 0.003	0.10	30
10.2	14	-186 ± 1	-33 ± 1	0.842 ± 0.002	0.09	33
10.2	14	-188 ± 1	-32 ± 2	0.839 ± 0.001	0.09	32
15.3	14	-180 ± 4	-26 ± 2	0.842 ± 0.004	0.09	34
15.3	14	-178 ± 1	-26 ± 1	0.845 ± 0.001	0.09	33
15.3	14	-179 ± 2	-25 ± 1	0.842 ± 0.002	0.08	36
20.4	14	-167 ± 1	-19 ± 2	0.849 ± 0.002	0.07	36
20.4	14	-167 ± 3	-19 ± 2	0.849 ± 0.004	0.08	35
20.3	14	-166 ± 2	-20 ± 2	0.851 ± 0.003	0.08	35
25.0	13	-154 ± 1	-11 ± 1	0.855 ± 0.001	0.09	36
25.0	13	-157 ± 1	-10 ± 2	0.852 ± 0.001	0.08	36
25.0	13	-155 ± 4	-12 ± 1	0.855 ± 0.004	0.08	36
30.0	13	-144 ± 1	-5 ± 2	0.860 ± 0.002	0.08	35
30.0	13	-147 ± 1	-5 ± 2	0.858 ± 0.002	0.09	34
30.0	13	-147 ± 2	-4 ± 2	0.857 ± 0.003	0.08	36
35.0	13	-131 ± 1	+4 ± 2	0.865 ± 0.002	0.07	39
34.9	13	-131 ± 1	+4 ± 2	0.865 ± 0.002	0.07	37
35.0	13	-134 ± 2	+5 ± 2	0.862 ± 0.003	0.07	37
10.2	35	-183 ± 2	-29 ± 1	0.842 ± 0.002	0.07	40
10.3	35	-184 ± 1	-31 ± 2	0.843 ± 0.002	0.07	41
10.2	35	-187 ± 1	-33 ± 2	0.840 ± 0.002	0.06	41
15.3	35	-178 ± 2[a]	-23 ± 1	0.841 ± 0.002	0.08	37
15.3	35	-181 ± 2	-26 ± 2	0.841 ± 0.002	0.07	38
15.3	35	-182 ± 2	-25 ± 1	0.839 ± 0.002	0.07	38
20.5	35	-173 ± 1	-18 ± 2	0.842 ± 0.002	0.07	39
20.4	35	-171 ± 1	-16 ± 2	0.842 ± 0.002	0.07	38
20.5	35	-171 ± 1	-19 ± 2	0.844 ± 0.002	0.07	40
25.1	35	-161 ± 3[a]	-11 ± 1	0.849 ± 0.003	0.07	39
25.1	35	-162 ± 2	-9 ± 2	0.846 ± 0.002	0.07	42
25.1	35	-162 ± 1	-11 ± 1	0.847 ± 0.001	0.07	41
30.2	35	-148 ± 1	-6 ± 2	0.857 ± 0.002	0.07	41
30.2	35	-152 ± 1	-6 ± 2	0.853 ± 0.002	0.07	42
30.2	35	-150 ± 1	-3 ± 2	0.853 ± 0.002	0.07	43
35.2	35	-136 ± 3	+4 ± 2	0.860 ± 0.003	0.06	44
35.2	35	-136 ± 1[a]	+3 ± 2	0.861 ± 0.002	0.06	42
35.2	35	-134 ± 1	+5 ± 3	0.862 ± 0.002	0.06	41

[a] Mean of triplicate measurement ± 1 standard deviation